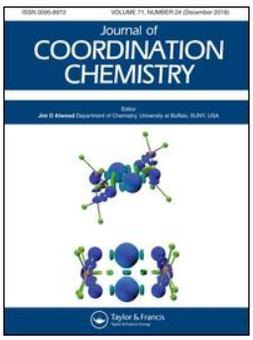

Taylor & Francis
Taylor & Francis Group

Journal of Coordination Chemistry

ISSN: (Print) (Online) Journal homepage: https://www.tandfonline.com/loi/gcoo20

Some new Cu(II) complexes containing O,N-donor Schiff base ligands derived from 4-aminoantipyrine: synthesis, characterization, crystal structure and substitution effect on antimicrobial activity

Hadi Kargar, Fariba Aghaei-Meybodi, Mohammad Reza Elahifard, Muhammad Nawaz Tahir, Muhammad Ashfaq & Khurram Shahzad Munawar

To cite this article: Hadi Kargar, Fariba Aghaei-Meybodi, Mohammad Reza Elahifard, Muhammad Nawaz Tahir, Muhammad Ashfaq & Khurram Shahzad Munawar (2021): Some new Cu(II) complexes containing O,N-donor Schiff base ligands derived from 4-aminoantipyrine: synthesis, characterization, crystal structure and substitution effect on antimicrobial activity, Journal of Coordination Chemistry, DOI: 10.1080/00958972.2021.1900831

To link to this article: https://doi.org/10.1080/00958972.2021.1900831

JOURNAL OF COORDINATION CHEMISTRY
https://doi.org/10.1080/00958972.2021.1900831

Some new Cu(II) complexes containing O,N-donor Schiff base ligands derived from 4-aminoantipyrine: synthesis, characterization, crystal structure and substitution effect on antimicrobial activity

Hadi Kargar[a], Fariba Aghaei-Meybodi[b], Mohammad Reza Elahifard[c], Muhammad Nawaz Tahir[d], Muhammad Ashfaq[d] and Khurram Shahzad Munawar[e,f]

[a]Department of Chemical Engineering, Faculty of Engineering, Ardakan University, Ardakan, Iran; [b]Department of Chemistry, Payame Noor University, Tehran, Iran; [c]Department of Metallurgical Engineering, University of Nevada, Reno, NV, USA; [d]Department of Physics, University of Sargodha, Punjab, Pakistan; [e]Department of Chemistry, University of Sargodha, Punjab, Pakistan; [f]Department of Chemistry, University of Mianwali, Mianwali, Pakistan

ABSTRACT

A new series of mononuclear Cu(II) complexes, $[Cu(L^1)_2]$: C1, $[Cu(L^2)_2]$: C2, $[Cu(L^3)_2]$: C3 and $[Cu(L^4)_2]$: C4, with *bis*-O, N-bidentate Schiff base ligands (H**L**^{1}: (*E*)-4-[(2-hydroxy-5-bromobenzylidene)amino]-1,5-dimethyl-2-phenyl-1,2-dihydro-3*H*-pyrazol-3-one; H**L**^{2}: (*E*)-4-[(2-hydroxy-5-chlorobenzylidene)amino]-1,5-dimethyl-2-phenyl-1,2-dihydro-3*H*-pyrazol-3-one; H**L**^{3}: (*E*)-4-[(2-hydroxy-5-hydroxybenzylidene)amino]-1,5-dimethyl-2-phenyl-1,2-dihydro-3*H*-pyrazol-3-one; H**L**^{4}: (*E*)-4-[(2-hydroxy-5-nitrobenzylidene)amino]-1,5-dimethyl-2-phenyl-1,2-dihydro-3*H*-pyrazol-3-one) have been prepared and characterized by elemental (CHN) analyses, FT-IR and multinuclear NMR (^{1}H and ^{13}C) spectroscopy. Furthermore, the crystal structures of H**L**^{3}, H**L**^{4} and **C4** were analyzed by single-crystal X-ray diffraction (SC-XRD). The XRD studies revealed that **C4** has 2:1 ligand-to-metal ratio and adapts highly distorted square planar geometry. The *in vitro* antibacterial activities of the synthesized ligands and their respective copper(II) complexes were elaborated by screening them against *Staphylococcus aureus* and *Escherichia coli*. The results showed a wide range of antimicrobial activity due to different electronic environments of the substituents on phenolic moiety.

ARTICLE HISTORY
Received 24 September 2020
Accepted 24 February 2021

KEYWORDS
Aminoantipyrine; Schiff base complex; x-ray structure; antibacterial activity

CONTACT Hadi Kargar h.kargar@ardakan.ac.ir; hadi_kargar@yahoo.com Department of Chemical Engineering, Faculty of Engineering, Ardakan University, P.O. Box 184, Ardakan, Iran.

Supplemental data for this article is available online at https://doi.org/10.1080/00958972.2021.1900831.

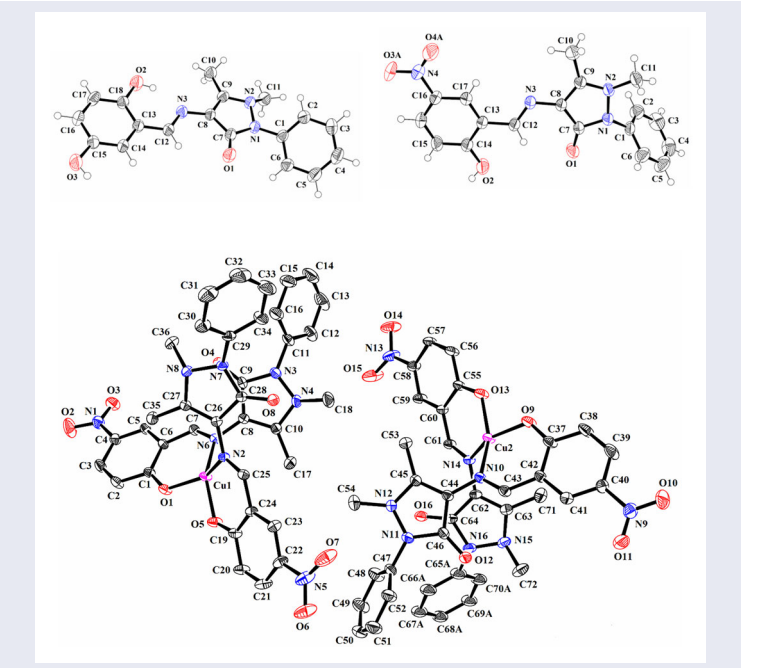

1. Introduction

Nowadays, an emergency medical issue is the increasing resistance of microbes against commonly available antibiotics which leads to the synthesis of new novel antimicrobial compounds that can be proved to have potential against these mutated pathogens [1–3]. Schiff bases are considered promising precursors for the synthesis of new bioactive compounds of medicinal relevance due to their biological as well as pharmacological importance and ability to form chelates with transition metals [4–8]. Schiff bases are not only good σ-donors but also very excellent π-acid ligands, as these have the ability to accept the electronic density into empty π^*-antibonding molecular orbitals of HC = N (azomethine group) from metal possessing low oxidation states. The Schiff bases, with the aid of phenolic group at *ortho*-position, can act as monobasic bidentate ligands in nature and make the basis of coordination chemistry with a variety of metals [9–11].

Schiff base derivatives of 4-aminoantipyrine have a dominant position in medicinal chemistry due to their wide spectrum of applications like antituberculosis, antineoplastic, antimalarial, anticancer, antioxidant, antifungal, anti-inflammatory, anti-proliferative activity and corrosion inhibition [12–15]. Antipyrine can also coordinate with the metal ions in a monodentate fashion *via* its carbonyl oxygen [16]. Coordination of metal with ligand brings matchless improvement in the biological properties of not only the ligand but also the metal ion [17–19]. The most suitable metals, specifically for this motive, are transition metals as they can adapt to extensive types of coordination

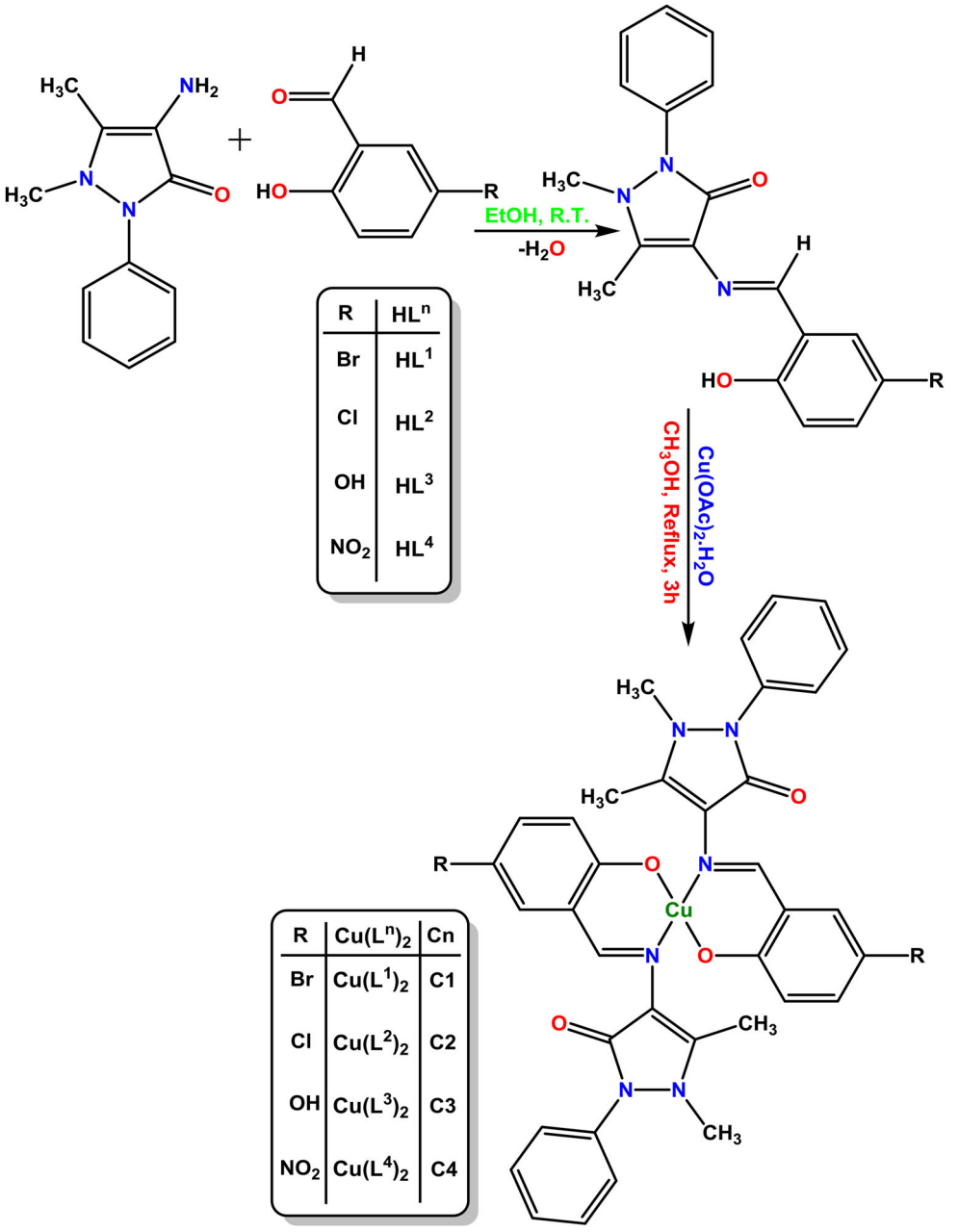

Scheme 1. The synthesis pathways of ligands HL^1–HL^4 and complexes **C1–C4**.

numbers, geometries and oxidation states as compared to carbon and other main group elements.

Copper complexes can exhibit astonishing pharmacological potential, which are not observed when the ligand or simple inorganic salts of copper are used alone [20–23]. It is revealed from the literature that a very limited number of copper(II) complexes

are reported with O- and N-donor Schiff bases derived from 4-aminoantipyrine [24]. Furthermore, no work is done pointing out the comparative analysis of substitution effect of various moieties on the salicylaldehydic part of the Schiff base derived from 4-aminoantipyrine and its respective Cu(II) complexes on the antibacterial activities.

This triggers us to prepare a new series of bioactive Cu(II) complexes with four bidentate (O,N) Schiff bases derived by the condensation of 4-aminoantipyrine with *para*-substituted salicylaldehyde. Moreover, these synthesized compounds were characterized by various analytical and spectroscopic techniques and then screened for their antibacterial activities.

2. Experimental

2.1. Materials and methods

All materials were purchased commercially from Merck and used without purification. FT-IR spectra were recorded on an IR Prestige-21 spectrophotometer from 400 to 4000 cm^{-1} using KBr pellets. ^{1}H and ^{13}C NMR spectra of the ligands were recorded at ambient temperature with a Bruker Avance 400 MHz spectrometer. Elemental (CHN) analyses were performed using a Heraeus CHN-O-FLASH EA 1112 elemental analyzer. X-ray data was recorded by a Bruker KAPPA APEXII CCD X-ray diffractometer.

2.2. Synthesis of Schiff base ligands (HL^n) (n = 1–4)

For the preparation of bidentate Schiff bases (HL^n), an equimolar (1:1) solution of 1-phenyl-2,3-dimethyl-4-amino-3-pyrazolin-5-one (0.203 g, 1 mM) in ethanol (10 mL) and respective salicylaldehyde [(0.201 g, 1 mM), 5-bromosalicylaldehyde for HL^1 (0.156 g, 1 mM), 5-chlorosalicylaldehyde for HL^2 (0.138 g, 1 mM), 5-hydroxysalicylaldehyde for HL^3 and (0.167 g, 1 mM), 5-nitrosalicylaldehyde for HL^4] in ethanol (20 mL) were mixed and stirred for 1 h at room temperature to get a clear yellow solution. Afterwards, the solution was covered with aluminum foil and kept in air for slow evaporation for a period of 5 days to collect yellow prism-shaped crystals of HL^3 and HL^4 and yellow precipitates of HL^1 and HL^2. The synthesized products were filtered and washed with ethanol to remove any impurity and finally dried in air. The elemental analyses, ^{1}H NMR, ^{13}C NMR and FT-IR data clearly confirmed their composition. The synthesis of the ligands is illustrated in Scheme 1.

(*E*)-4-[(2-hydroxy-5-bromobenzylidene)amino]-1,5-dimethyl-2-phenyl-1,2-dihydro-3*H*-pyrazol-3-one, HL^1; Yield: 78%. Anal. Calcd for $C_{18}H_{16}BrN_3O_2$: C, 55.97; H, 4.18; N, 10.88%. Found: C, 55.68; H, 4.09; N, 10.97. FT-IR (KBr, cm^{-1}): ν(C = O) 1637, ν(C = N) 1595, ν(C-O) 1124. ^{1}H NMR ($CDCl_3$, 400 MHz, 298 K), δ (ppm): 2.44 (s, 3H, $–CH_3$-C); 3.22 (s, 3H,$–CH_3$-N); 6.86 (d, $^{3}J = 8.8$ Hz, H_c); 7.37 (dd, $^{3}J = 8.8$ Hz, $^{4}J = 2.4$ Hz, H_b); 7.46 (d, $^{4}J = 2.4$ Hz, H_a); 7.39–7.54 (m, 5H, antipyrine ring); 9.76 (s, –CH = N, H_i); 13.41 (s, –OH, H_p). ^{13}C NMR ($CDCl_3$, 100 MHz, 298 K), δ (ppm): 10.32; 35.55; 110.63; 115.83; 118.68; 121.75; 124.82; 127.54; 129.41; 133.85; 134.17; 134.35; 149.89; 158.87; 159.44.

(*E*)-4-[(2-hydroxy-5-chlorobenzylidene)amino]-1,5-dimethyl-2-phenyl-1,2-dihydro-3*H*-pyrazol-3-one, HL^2; Yield: 81%. Anal. Calcd for $C_{18}H_{16}ClN_3O_2$: C, 63.25; H, 4.72; N, 12.29%. Found: C, 63.08; H, 4.67; N, 12.47. FT-IR (KBr, cm^{-1}): ν(C = O) 1637, ν(C = N)

1595, ν(C-O) 1122. ^{1}H NMR ($CDCl_3$, 400 MHz, 298 K), δ (ppm): 2.44 (s, 3H, –CH_3-C); 3.23 (s, 3H,–CH_3-N); 6.91 (d, $^{3}J = 8.8$ Hz, H_c); 7.24 (dd, $^{3}J = 8.8$ Hz, $^{4}J = 2.6$ Hz, H_b); 7.32 (d, $^{4}J = 2.6$ Hz, H_a); 7.38–7.54 (m, 5H, antipyrine ring); 9.77 (s, –CH = N, H_i); 13.37 (s, –OH, H_p). ^{13}C NMR ($CDCl_3$, 100 MHz, 298 K), δ (ppm): 10.32; 35.55; 110.83; 117.73; 118.22; 124.81; 127.54; 129.40; 130.87; 131.54; 134.38; 134.75; 149.97; 159.01; 160.07.

(*E*)-4-[(2-hydroxy-5-hydroxybenzylidene)amino]-1,5-dimethyl-2-phenyl-1,2-dihydro-3*H*-pyrazol-3-one, H**L^{3}**; Yield: 69%. Anal. Calcd for $C_{18}H_{17}N_3O_3$: C, 66.86; H, 5.30; N, 13.00%. Found: C, 66.64; H, 5.37; N, 12.89. FT-IR (KBr, cm^{-1}): ν(C = O) 1651, ν(C = N) 1587, ν(C-O) 1139. ^{1}H NMR (DMSO-*d*^{6}, 400 MHz, 298 K), δ (ppm): 2.39 (s, 3H, –CH_3-C); 3.20 (s, 3H,–CH_3-N); 6.74 (br, H_c); 6.75 (br, H_b); 6.83 (d, $^{4}J = 2.0$ Hz, H_a); 7.37–7.56 (m, 5H, antipyrine ring); 9.01 (s, –CH = N, H_i); 9.60 (s, –OH, H_q); 12.07 (s, –OH, H_p). ^{13}C NMR (DMSO-*d*^{6}, 100 MHz, 298 K), δ (ppm): 9.80; 35.15; 115.50; 116.94; 119.34; 120.20; 124.85; 127.18; 129.18; 134.19; 149.65; 150.27; 152.13; 157.12; 159.13.

(*E*)-4-[(2-hydroxy-5-nitrobenzylidene)amino]-1,5-dimethyl-2-phenyl-1,2-dihydro-3*H*-pyrazol-3-one, H**L^{4}**; Yield: 73%. Anal. Calcd for $C_{18}H_{16}N_4O_4$: C, 61.36; H, 4.58; N, 15.90%. Found: C, 61.12; H, 4.66; N, 15.78. FT-IR (KBr, cm^{-1}): ν(C = O) 1649, ν(C = N) 1593, ν(C-O) 1139. ^{1}H NMR ($CDCl_3$, 400 MHz, 298 K), δ (ppm): 2.47 (s, 3H, –CH_3-C); 3.27 (s, 3H,–CH_3-N); 7.03 (d, $^{3}J = 9.1$ Hz, H_c); 8.20 (dd, $^{3}J = 9.1$ Hz, $^{4}J = 2.7$ Hz, H_b); 8.32 (d, $^{4}J = 2.7$ Hz, H_a); 7.39–7.56 (m, 5H, antipyrine ring); 9.89 (s, –CH = N, H_i); 14.48 (s, –OH, H_p). ^{13}C NMR ($CDCl_3$, 100 MHz, 298 K), δ (ppm): 10.33; 35.37; 117.56; 119.49; 125.08; 127.08; 127, 64; 127.85; 129.51; 133.91; 140.18; 149.64; 157.96; 159.91; 165.95.

2.3. Synthesis of the copper(II) complexes

Copper(II) complexes of the type [Cu(**L^{n}**)$_2$] (**C1–C4**), where **L^{n}** = **L^{1}–L^{4}**, with four bidentate Schiff base ligands (H**L^{n}**) were prepared by adding metal precursor $Cu(OAc)_2{\cdot}H_2O$ (0.200 g, 1 mM) to a hot solution of the corresponding ligand H**L^{n}** (2.0 mM) in methanol (30 mL). The mixture was refluxed for 3 h and then resultant suspension was filtered, washed thoroughly with methanol and then finally dried in air. Black-green crystals of **C4** suitable for X-ray measurements were obtained from methanol solution. The synthesis of the complexes is also illustrated in Scheme 1.

C1; [Cu(L^{1})$_2$], Yield: 67%. Anal. Calcd for $C_{36}H_{30}Br_2CuN_6O_4$: C, 51.84; H, 3.63; N, 10.08%. Found: C, 51.67; H, 3.69; N, 10.29. FT-IR (KBr, cm^{-1}): ν(C = O) 1651, 1606; ν(C = N) 1589; ν(C-O) 1246.

C2; [Cu(L^{2})$_2$], Yield: 75%. Anal. Calcd for $C_{36}H_{30}Cl_2CuN_6O_4$: C, 58.03; H, 4.06; N, 11.28%. Found: C, 57.89; H, 4.14; N, 11.17. FT-IR (KBr, cm^{-1}): ν(C = O) 1649, 1606; ν(C = N) 1587; ν(C-O) 1315.

C3; [Cu(L^{3})$_2$], Yield: 58%. Anal. Calcd for $C_{36}H_{32}CuN_6O_6$: C, 61.05; H, 4.55; N, 11.87%. Found: C, 60.87; H, 4.61; N, 11.75. FT-IR (KBr, cm^{-1}): ν(C = O) 1654, 1606; ν(C = N) 1560; ν(C-O) 1276.

C4; [Cu(L^{4})$_2$], Yield: 64%. Anal. Calcd for $C_{36}H_{30}CuN_8O_8$: C, 56.43; H, 3.95; N, 14.62%. Found: C, 56.27; H, 4.03; N, 14.56. FT-IR (KBr, cm^{-1}): ν(C = O) 1654, 1600; ν(C = N) 1543; ν(C-O) 1240.

2.4. Crystal structure determination

The X-ray diffraction measurements of compounds H**L**^{3}, H**L**^{4} and **C4** were carried out on a Bruker Kappa APEXII CCD X-ray diffractometer with graphite monochromated Mo-Kα radiation (λ = 0.71073 Å). The single-crystals suitable for X-ray analysis were obtained from methanol solution and mounted on a glass fiber for data collection using Bruker Apex-II software [25]. The structures were solved by direct methods and subsequent difference Fourier maps on SHELXS97 [26] and then refined on F^2 by a full-matrix least-squares procedure using anisotropic displacement parameters. Atomic factors are taken from the international tables for X-ray Crystallography [27]. All non-hydrogen atoms were refined with anisotropic displacement parameters. Hydrogens were placed in ideal positions and refined as riding atoms with relative isotropic displacement parameters. All refinements were performed using SHELXL-2018/3 and WinGX-2014.1 programs [28, 29]. The method to collect data was ω-scans and integrated using Bruker SAINT [30] software package. The crystallographic illustrations for H**L**^{3}, H**L**^{4} and **C4** were prepared using ORTEP-3 [29] and Platon [31]. Experimental parameters pertaining to single-crystal X-ray analysis of compounds are given in Table S1.

2.5. Antibacterial activity

In vitro antibacterial activities of the Schiff base ligands and their copper(II) complexes were assessed against both gram-positive and gram-negative bacteria. Herein, *Escherichia coli* (*E. coli*, ATCC 25922) and *Staphylococcus aureus* (*S. aureus*, ATCC 25923), common referenced gram-negative and gram-positive bacteria, respectively, were examined. Using dilution method, the lowest level of antimicrobial agent that greatly inhibits the growth of a microorganism, Minimum Inhibitory Concentration (MIC), and the lowest level of antimicrobial agent resulting in microbial death, Minimum Bactericidal Concentration (MBC), were recorded. The mixtures of 1024, 512, 256, 128, 64, 32, 16, 8, 4 and 2 μg/mL of antibacterial agents (free ligands, their complexes and Streptomycin as internal standard) with suspension of 5×10^5 CFU/mL of test strains (0.5 McFarland) in Muller-Hinton broth (MHB) were provided in 96-well plates. It also included one growth control (MHB) and one sterility control (MHB + compound). After incubation at 37 °C for 18–24 h, the MIC for each tested substance was indicated by the presence of a white "pellet" on the bottom of the well. The dilution representing the MIC and three more concentrated suspensions were plated and enumerated to determine viable CFU/mL as MBC value. It is the lowest concentration of a substance necessary to achieve a bactericidal effect that demonstrates a pre-determined reduction (99.9%) in CFU/mL when compared to the MIC dilution.

3. Results and discussion

3.1. Synthesis

Condensation of 4-aminoantipyrine with equimolar amounts of the respective *para*-substituted salicylaldehydes leads to the formation of an important class of bidentate

Table 1. Selected bond bond lengths (Å) and angles (°) for HL^3, HL^4 and C4.

Selected bond lengths for HL^3		Selected bond lengths for HL^4	
C7-C8	1.442(4)	C7-C8	1.434(2)
C8-N3	1.399(3)	C8-N3	1.394(2)
C12-N3	1.292(3)	C12-N3	1.272(2)
C12-C13	1.446(4)	C12-C13	1.446(2)
Selected bond angles for HL^3		Selected bond angles for HL^4	
C7-C8-N3	129.1(2)	C7-C8-N3	129.6(1)
C8-N3-C12	122.2(2)	C8-N3-C12	119.89(2)
N3-C12-C13	120.8(3)	N3-C12-C13	121.7(1)
Selected bond lengths for molecule I of C4		Selected bond lengths for molecule II of C4	
Cu1-O1	1.907(2)	Cu2-O9	1.903(2)
Cu1-O5	1.878(2)	Cu2-O13	1.884(2)
Cu1-N2	1.949(2)	Cu2-N10	1.968(2)
Cu1-N6	1.954(2)	Cu2-N14	1.964(3)
Selected bond angles for molecule I of C4		Selected bond angles for molecule II of C4	
O5-Cu1-O1	91.73(10)	O13-Cu2-O9	90.73(10)
O5-Cu1-N2	148.57(11)	O13-Cu2-N10	153.88(12)
O1-Cu1-N2	94.66(10)	O9-Cu2-N10	93.02(10)
O5-Cu1-N6	94.00(10)	O13-Cu2-N14	93.13(10)
O1-Cu1-N6	143.90(11)	O9-Cu2-N14	150.64(12)
N2-Cu1-N6	98.66(10)	N14-Cu2-N10	96.12(10)

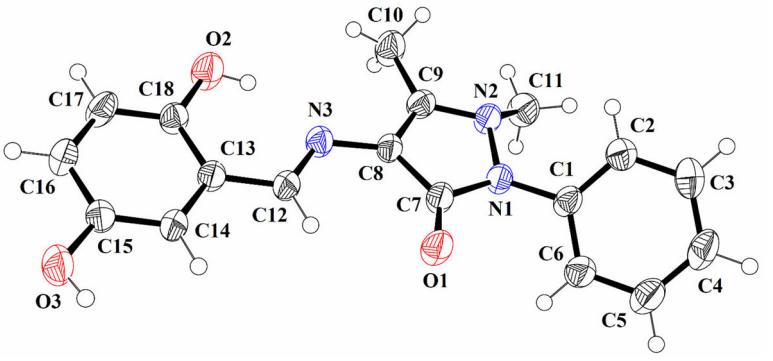

Figure 1. ORTEP diagram of HL^3 drawn at the probability level of 50%. H-atoms are shown by small circles of arbitrary radii.

Schiff base ligands. Treatment of the Schiff base ligands HL^{1-4} with the respective $Cu(OAc)_2{\cdot}H_2O$ in a 2:1 ratio under reflux led to the formation of copper(II) complexes (**C1–C4**). The spectroscopic data are in agreement with the chemical formula proposed for Schiff base complexes. The synthetic procedure for the Schiff base ligands and their copper complexes is presented in Scheme 1.

3.2. Crystal structures of HL^3, HL^4 and C4

In HL^3 (Figure 1, Table S1), the benzene ring of the 4-amino-1,5-dimethyl-2-phenyl-1H-pyrazol-3(2H)-one moiety i.e., A (C1-C6), the 4-amino-1H-pyrazol-3(2H)-one ring B (C7-C9/N1-N3/O1) and 2-methylbenzene-1,4-diol group C (C12-C18/O2/O3) are planar with r.m.s deviations of 0.0075, 0.0365 and 0.0189 Å, respectively. The C-atoms (C10/C11)

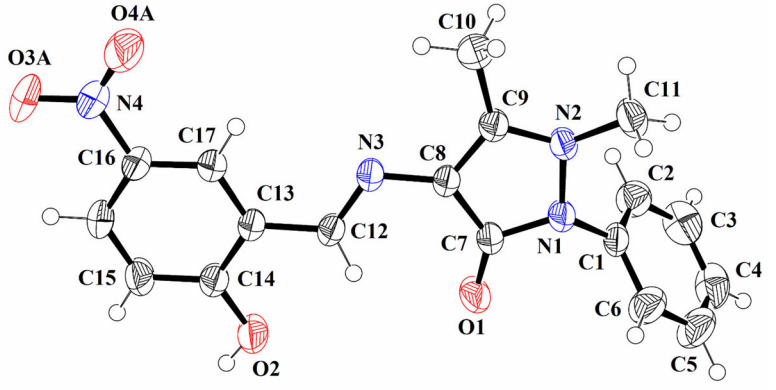

Figure 2. ORTEP diagram of HL^4 drawn at the probability level of 50%. H-atoms are shown by small circles of arbitrary radii.

Table 2. Characteristic ^{1}H NMR chemical shift values (ppm), peak multiplicity and coupling constant J (Hz) for the synthesized compounds recorded in $CDCl_3$ (except HL^3, which was recorded in DMSO-d^6).

Compound	$-CH_3$-C	$-CH_3$-N	H_c	H_b	H_a	Antipyrine ring (5 H)	H_i	H_p
HL^1	2.44 s	3.22 s	6.86 d $J = 8.8$	7.37 dd $J = 8.8; 2.4$	7.46 d $J = 2.4$	7.39-7.54 m	9.76 s	13.41 s
HL^2	2.44 s	3.23 s	6.91 d $J = 8.8$	7.24 dd $J = 8.8; 2.6$	7.32 d $J = 2.6$	7.38-7.54 m	9.77 s	13.37 s
HL^3	2.39 s	3.20 s	6.74 br	6.75 br	6.83 d $J = 2.0$	7.37-7.56 m	9.01 s	12.07 s
HL^4	2.47 s	3.27 s	7.03 d $J = 9.1$	8.20 dd $J = 9.1; 2.7$	8.32 d $J = 2.7$	7.39-7.56 m	9.89 s	14.48 s

Table 3. Characteristic ^{13}C NMR chemical shift values (ppm) for the synthesized compounds recorded in $CDCl_3$ (except HL^3, which was recorded in DMSO-d^6).

Compound	$-CH_3$-C	$-CH_3$-N	Aromatic and pyrazoline ring carbons	$-C=O$	$-C=N$
HL^1	10.32	35.55	110.63-149.89	158.87	159.44
HL^2	10.32	35.55	110.83-149.97	159.01	160.07
HL^3	9.80	35.15	116.94-152.13	157.12	159.13
HL^4	10.33	35.37	117.56-157.96	159.91	165.95

are deviated from the plane of ring B and are at the distance of −0.0127(5) and −0.5884(5) Å, respectively, below the plane of ring B. The dihedral angles for A/B, A/C and B/C are 45.4(8)°, 47.4(8)° and 5.47(1)°, respectively. This dihedral angle investigation inferred that ring B and group C are almost parallel to each other. The dihedral angle between phenyl ring (C1-C6) of antipyrine group and central five-membered ring is 43.8(1)° as compared to 49.67° and 36.64° between similar rings in already reported similar crystal structures having different substitution at the benzene ring [32]. Selected bond lengths and angles are given in Table 1. The hydroxyl group in ortho-position interacts with imine N-atom through intra O-H … N bonding to form an S(6) loop as shown in Figure S1 and given in Table S2. Similar kind of intramolecular H-bonding is found in already reported Schiff base compounds having 2-hydroxy-3-bromo-4-chlorophenyl rings instead of 2,5-dihydroxyphenyl moiety [33]. The molecules are interlinked through strong O-H···O bonding to form C(7) chain, where O-atom of

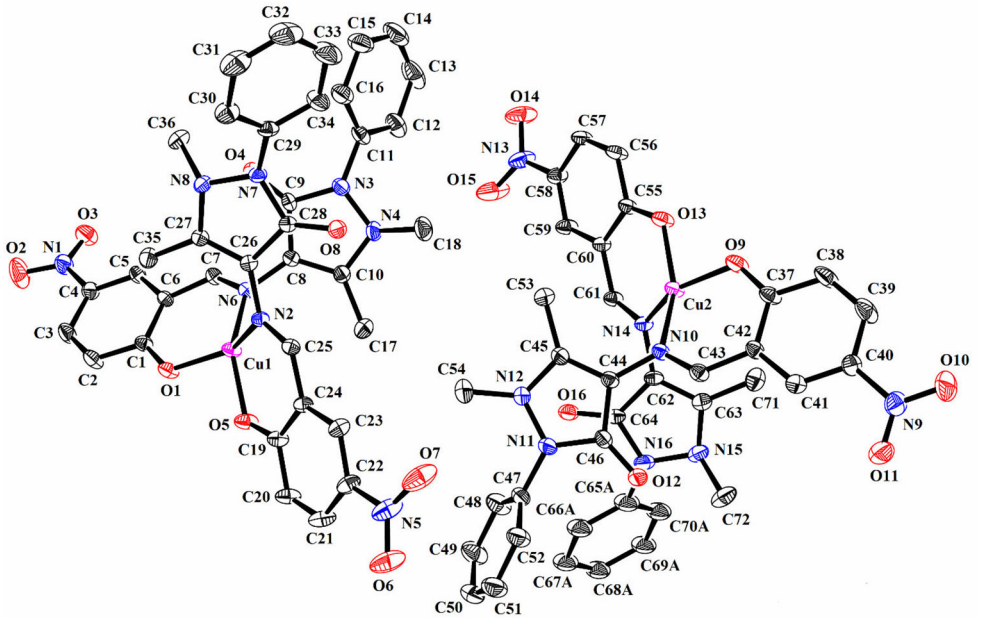

Figure 3. ORTEP diagram of **C4** drawn at the probability level of 20%. H-atoms are not shown for clarity.

meta-positioned hydroxyl group acts as donor and O-atom of *ortho*-positioned hydroxyl group acts as acceptor. The molecules are also interlinked through comparatively weak C-H···O bonding to form $R_2^1(7)$ loop, where CH from methyl group that is directly attached with N-atom of 2,3-dihydro-1H-pyrazole ring acts as donor whereas acceptor O-atom is from carbonyl group. The CH of other methyl group is also engaged in C-H···O bonding in which acceptor O-atom is from the *meta*-positioned hydroxyl group. The crystal packing is further stabilized by the presence of off-set π···π stacking interaction. The five-membered 2,3-dihydro-1H-pyrazole ring at asymmetric position is engaged in parallel off-set π···π stacking interaction with the phenyl ring of hydroquinone moiety at (-x, 2-y, -z). The centroid-to-centroid distance between these rings is 4.071 Å with ring offset of 2.087 Å, as shown in Figure S2 and given in Table S3. Similarly, inversion related phenyl rings of hydroquinone moiety are involved in parallel off-set π···π stacking interaction with centroid-to-centroid separation of 4.159 Å having ring off-set of 2.388 Å. The crystal packing of a related crystal structure having 2-hydroxy-4-methyoxy substituted phenyl ring instead of 2,5-dihydroxy substituted phenyl ring is stabilized by off-set π···π stacking interaction with inter-centroid separation ranges from 3.34 Å to 3.83 Å as found in literature [34].

In H**L**^{4} (Figure 2, Table S1), the benzene ring of the 4-amino-1,5-dimethyl-2-phenyl-1H-pyrazol-3(2H)-one moiety i.e., A (C1-C6), the ring B (C7-C9/N1-N3/O1) and o-cresol group C (C12-C18/O2) are planar with r.m.s deviations of 0.0053, 0.0387 and 0.0074 Å, respectively. The C-atoms (C10/C11) are deviated from the plane of ring B and are at the respective distances of 0.0486(2) and 0.4540(2) Å. The O-atoms of nitro group are disordered over two sets of sites with occupancy ratio 0.886(13): 0.114(13). The major

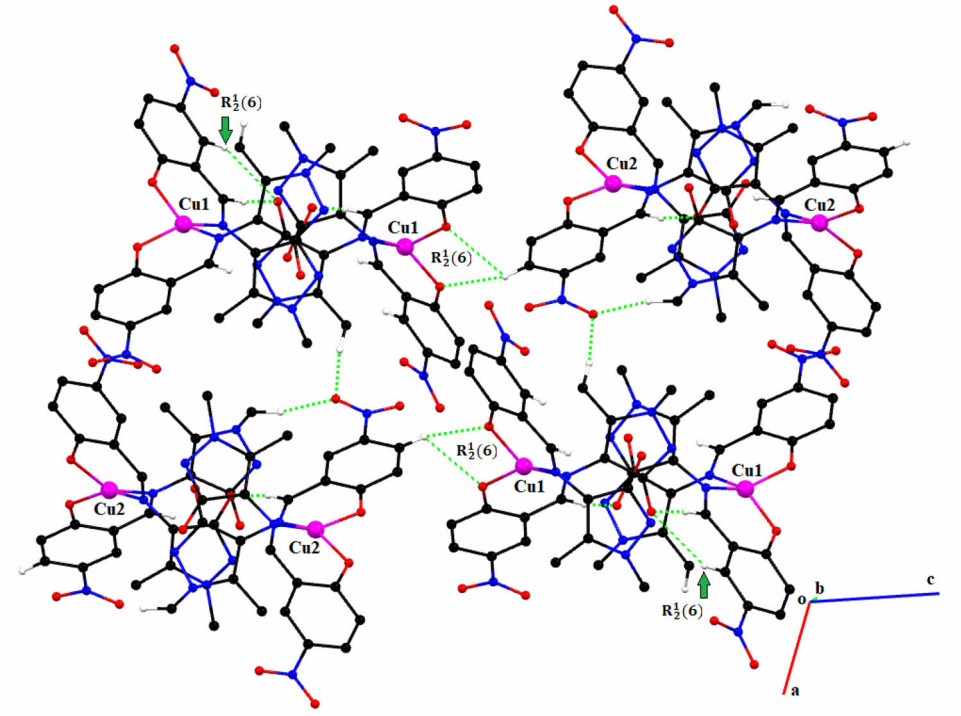

Figure 4. Packing diagram of **C4**. H-atoms not involved in H-bonding are omitted for clarity. Benzene rings attached to 1,5-dimethyl-1H-pyrazol-3(2H)-one rings are not involved in H-bonding are also omitted for clarity.

part of nitro group D (N4/O3A/O4A) and minor part of nitro group E (N4/O3B/O4B) are twisted at the dihedral angle of 54.9(3)° with respect to each other. The dihedral angles for A/B, A/C, B/C, C/D and C/E are 67.6(5)°, 72.6(5)°, 5.13(6)°, 7.74(6)° and 48.56(2)°, respectively. The investigation of dihedral angles revealed that ring B and group C are almost parallel to each other. Selected bond lengths and angles are given in Table 1. The molecules are first connected with each other in the form of dimers through strong O-H···O bonding to form $R_2^2(18)$ loop, where acceptor O-atom is from the carbonyl group as shown in Figure S3. One of the CH of benzene ring (C1-C6) acts as a donor for both parts of one of the O-atoms of the nitro group to interlink molecules with each other as given in Table S2. The major part of the other O-atom of nitro group is also involved in comparatively weak C-H···O bonding, where CH is from benzene ring (C1-C6). The minor part of the same O-atom is also involved in C-H···O bonding, where CH is from one methyl group connected with the N-atom of the 4-amino-1H-pyrazol-3(2H)-one ring. The crystal packing is further stabilized by the presence of off-set π···π stacking interaction. The five-membered 2,3-dihydro-1H-pyrazole ring (C7-C9/N1/N2) is engaged in parallel off-set π···π stacking interaction with the benzene ring (C1-C6) with centroid-to-centroid distance of 3.632 Å having ring off-set of 1.032 Å, as shown in Figure S4 and given in Table S3. These rings are connected by inversion symmetry. The crystal packing of H**L**^{4} is entirely different from already reported very similar crystal structure having 2,4-dihydroxy substituted benzene ring

Table 4. FT-IR spectral data of the ligands and their corresponding copper(II) complexes (cm^{-1}).

	HL^1	C1	HL^2	C2	HL^3	C3	HL^4	C4
v(C = N)	1595	1589	1595	1587	1587	1560	1593	1543
v(C–O)	1124	1246	1122	1315	1139	1276	1139	1240
v(Cu–N)	—	410	—	443	—	422	—	420
v(Cu–O)	—	547	—	547	—	549	—	557

Table 5. MIC and MBC of the ligands and their corresponding copper(II) complexes.

	MIC (μg/mL)		MBC (μg/mL)	
Compound	*E. coli*	*S. aureus*	*E. coli*	*S. aureus*
HL^1	512	256	—	—
HL^2	512	256	—	—
HL^3	256	128	—	1024
HL^4	256	64	1024	512
C1	128	64	512	256
C2	128	128	512	256
C3	64	64	256	128
C4	64	32	128	64
Streptomycin	8	4	32	16

instead of 2,5-dihydroxy substituted benzene ring because in the crystal packing of the former compound, the substituted benzene ring is stabilized by C-H···N bonding in addition to O-H···O bonding whereas in HL^4 C-H···N bonding is absent [32].

In **C4** (Figure 3, Table S1), there are two crystallographically independent molecules **I** (C1-C36/N1-N8/O1-O8/Cu1) and **II** (C37-C72/N9-N16/O9-O16/Cu2) in the asymmetric unit. Selected bond lengths and angles for molecules **I** and **II** are displayed in Table 1. In both molecules, ligand-to-metal ratio is 2:1, and the coordination sphere around the central Cu-atom consists of two N-atoms and two O-atoms with both ligands chelating the central Cu-atom in a *cis* arrangement as compared to *trans* arrangement of ligands in already reported similar structure having methoxy-substituted phenyl ring instead of nitro-substituted phenyl ring [35]. Similar ligand-to-metal ratio is also found in related crystal structure [36]. The distance of Cu1 atom to the basal plane defined by (N2/N6O1/O5) is 0.66 Å whereas the distance of Cu2 to the basal plane defined by (N10/N14/O9/O13) is 0.23 Å as compared to the distance value of 0.03 Å and 0.050 Å of the copper atom from a similar basal plane in already reported similar structures with different chelating ligands [36, 37]. The geometry of **C4** can be computed with the help of the τ_4 geometry index, $\tau_4 = [360 - (\alpha + \beta)]/141$, where α and β are the two largest angles around the metal center. The value of τ_4 changes from 0 (perfect square planar) to 1 (regular tetrahedral) [38–40]. In **C4**, the geometries of molecules **I** and **II** are highly distorted square planar, as evident from the values of τ_4, 0.48 and 0.39, respectively. In molecule **I**, the dihedral angle among nitrobenzene rings A (C1-C6/N1/O2/O3) and B (C19-C24/N5/O6/O7) is 47.3(1)° whereas in molecule **II**, the dihedral angle between similar nitrobenzene rings C (C37-C42/N9/O10/O11) and D (C55-C60/N13/O14/O15) is 34.8(1)°. In molecule **I**, 2,3-dihydro-1H-pyrazole rings E (C8-C10/N3/N4) and F (C26-C28/N7/N8) are twisted at the dihedral angle of 16.4(1)° with respect to each other whereas in molecule **II**, dihedral angle between similar five-membered rings G (C44-C46/N11/N12) and H (C62-C64/N15/N16) is 16.2(3)°. In molecule **I**, phenyl rings I (C11-C16) and J (C29-C34) are planar with r.m.s deviations of 0.0036 and 0.0054 Å with dihedral angle I/J is 31.8(3)°. In molecule **II**, phenyl ring K

(C47-C52) is planar with r.m.s deviation of 0.0073 Å. The phenyl ring L (C65-C70) is disordered over three sets of sites with occupancy of 1/3 for each site. The molecules of type **I** are connected with each other in the form of dimers through C-H···O bonding to form a $R_2^1(6)$ loop as shown in Figure 4 and given in Table S2. In this C-H···O binding, O-atom attached to a 2,3-dihydro-1H-pyrazole ring E acts as a bifurcated acceptor. Molecules **I** and **II** are interlinked through C35-H35B···O15, C57-H57···O1 and C57-H57···O5 bonding whereas the molecules of type **II** are connected with each other through C43-H43···O16, C61-H61···O12 and C72-H72C···O15 bonding as specified in Table S2. No off-set $\pi \ldots \pi$ stacking interaction is found in the crystal packing of **C4**. Crystal packing of already reported similar copper complex having methoxy-substituted benzene ring instead of nitro-substituted benzene was stabilized by the presence of strong O-H···O bonding but in **C4**, no strong intermolecular O-H···O bonding is found [36].

3.3. NMR spectra

^{1}H NMR spectra of the ligands were recorded in deuterated chloroform-*d* (with the exception of H**L^3**, which was recorded in deuterated DMSO-d_6). The results are given in Table 2 and the spectra are shown in Figures S5-S8. The spectra displayed two sharp signals at 2.39–2.47 and 3.20–3.27 ppm with an integration equivalent to three hydrogen atoms corresponding to the $C-CH_3$ and $N-CH_3$ groups, respectively. The absorption peaks of salicylaldehyde ring protons (H_a, H_b and H_c) appeared within the expected range. The broadening in signals for the aromatic protons observed between 6.24 and 8.32 ppm indicate the presence of repeating aromatic units with a different chemical surrounding. The antipyrine aromatic rings give a group of multi signals at 7.37–7.56 ppm. The sharp singlets at $\delta = 9.01$–9.89 ppm are attributed to the H_i-C = N-proton of imine. The OH hydrogen for H**L^1**–H**L^4** resonates at $\delta = 13.41$, 13.37, 12.07 and 14.48 ppm as a sharp singlet, respectively.

The ^{13}C NMR spectra were recorded in the $CDCl_3$ (with the exception of H**L^3**, which was recorded in deuterated DMSO-d_6). The results are given in Table 3 and the spectra are shown in Figures S9–S12. The signals due to methyl carbons are observed around 10–35 ppm. The signals that appeared in the region $\delta = 110.6$–157.9 ppm are assigned to aromatic and pyrazoline ring carbons. The signals at $\delta = 157.1$–165.9 ppm are assigned to the carbonyl (C = O) and azomethine (HC = N) carbons, respectively.

3.4. FT-IR spectra

The measured FT-IR spectra of the ligands and their corresponding copper(II) complexes are shown in Figures S13–S21. Comparison between the selected bands in the FT-IR spectra of Schiff base ligands and their complexes are presented in Table 4 and Figure S21. In the FT-IR spectra for **C1**-**C4**, the ν(C = O) remains un-modified, indicating that the exocyclic ketonic oxygen of the antipyrine ring is not involved in the coordination while the ν(HC = N) and ν(C–O) bonds shifted to lower and higher wavenumbers, respectively, in comparison with their corresponding free ligands, thereby indicating a coordinative interaction of the iminic nitrogen and phenolic oxygen atoms

with Cu(II). The coordination of iminic nitrogen and phenolic oxygen could also be confirmed by the appearance of weak bands located at the low wavenumbers which are assigned to *v*(Cu–N) and *v*(Cu–O) at 410–443 cm^{-1} and 547–557 cm^{-1}, respectively. These results are consistent with structurally related compounds already reported [32, 34, 41].

3.5. Antibacterial activities

Having MIC and MBC measurements, antibacterial activities of the Schiff base ligands and their copper(II) complexes were executed and reported in Table 5. It is obvious from the results that a greater antibacterial activity of all tested compounds was observed against gram positive as compared to gram negative strains that is a normal trend of these kinds of antibacterial agents. Due to thinner peptidoglycan layers, gram-negative bacteria are protected from certain physical assaults because they do not absorb foreign materials that surround it, juxtaposition to this, thicker peptidoglycan layer of gram positive bacteria absorb antibiotics and cleaning products easily.

However, in comparison with a moderate antibacterial activity of free ligands, all complexes showed significant antibacterial activity against both *S. aureus* and *E. coli* under the same experimental conditions. The complexes provide bactericidal activities and inhibitory effects in a big range; MBC/MIC values of 512–128/128–64 μg/mL against *E. coli* and 256–64/128–32 μg/mL against *S. aureus*. Replacing R-group with methoxy to produce 1-phenyl-2,3-dimethyl-4-(N-2-hydroxy-4-meth-oxy-benzaldehyde)-3-pyrazolin-5-one, Rosu et al. [34] synthesized and evaluated antibacterial activity of six corresponded copper(II) complexes. In line with our results, they reported that the Schiff base has an inhibitory effect (MIC values in the range 128–512 μg/mL) on the growth of the *E. coli* and *S. aureus* strains and greater bactericidal activities against *E. coli* (MIC = 16–512 μg/mL) and *S. aureus* (MIC = 4–128 μg/mL) was observed for the complexes. Similarly, some complexes of Cu(II), Ni(II), VO(II) and Mn(II) with Schiff base derived from 4-amino-2,3-dimethyl-1-phenyl-3-pyrazolin-5-one showed a large range of inhibitory effects on the growth of the *E. coli* (MIC = 32–512 μg/mL) and *S. aureus* bacterial strains (MIC = 16–512 μg/mL) [42].

Herein, the MIC values of the synthesized free ligands are 512 and 128 μg/mL against *E. coli* and 256–64 μg/mL against *S. aureus*. Also, the MBC results of free ligands showed ignorable bactericidal activities, except H**L**^{4}. This behavior can be explained due to the formation of coordinate covalent bonds on the basis of Overtone's concept [43] and Tweedy's chelation theory [44]. Coordination reduces the polarity of the central metal ion, leading its larger atomic radius and electronegativity that decreases its effective positive charges and facilitates the interaction of complexes with cellular membranes which are highly sensitive towards the charged particle [45]. Moreover, the delocalization of π-electrons over the chelate ring system created by the donor groups during the coordination increases the lipophilicity of the complexes. It boosts their permeation through the lipid layer of the microorganism, thus destroying them more efficiently [46, 47].

Substituting only the R site, a wide range of inhibitory effects of the synthesized Schiff base ligands and corresponding complexes on the growth of the strains appears. The same trend of the different activity of the free ligands ($HL^4 > HL^3 > HL^2$ and HL^1) and their complexes (**C4** > **C3** > **C2** and **C1**) can be based on the electron-accepting feature of the substituents; stronger the electron acceptors (NO_2 > OH > Br and Cl), the higher will be the antibacterial activity.

4. Conclusion

A series of Schiff base ligands derived from 4-aminoantipyrine and their copper(II) complexes were synthesized and characterized by various physicochemical techniques. The exact molecular structures of ligands HL^3 and HL^4 and complex **C4** were determined by single-crystal X-ray crystallography. The X-ray structure of **C4** illustrates that the steric effect imposed by the methyl group has a profound influence on the Cu(II) geometry, rearranging into a distorted square planar shape. Even though the ligands are tridentate in nature, they coordinate with Cu(II) ion in a bidentate fashion through deprotonated phenolic oxygen and nitrogen of the azomethine chromophore, leaving the antipyrine exocyclic ketonic oxygen free. Having different electron-accepting features of substitutes, ligands and their complexes show a wide range of antimicrobial activities. The *in vitro* biological screening experiments resulted in higher activities for the complexes compared to the free Schiff base ligands. The activity data showed that the nitro-substituted Schiff base complex has a promising biological potential against all bacterial species.

Acknowledgements

The support of this work by Ardakan University and Payame Noor University are gratefully acknowledged. H.K. thanks Prof. Mehmet Akkurt from Erciyes University for the X-ray analysis of complex **C4**.

Disclosure statement

No potential conflict of interest was reported by the authors.

ORCID

Hadi Kargar http://orcid.org/0000-0002-7817-0937
Khurram Shahzad Munawar http://orcid.org/0000-0001-9055-2519

References

[1] F. Baquero. *J. Antimicrob. Chemother.*, **39**, 1 (1997).
[2] M.N. Alekshun, S.B. Levy. *Cell*, **128**, 1037 (2007).
[3] L.B. Rice. *Biochem. Pharmacol.*, **71**, 991 (2006).
[4] Z. Shokohi-Pour, H. Chiniforoshan, M.R. Sabzalian, S.-A. Esmaeili, A.A. Momtazi-Borojeni. *J. Biomol. Struct. Dyn.*, **36**, 532 (2018).

[5] K.S. Munawar, S. Ali, M.N. Tahir, N. Khalid, Q. Abbas, I.Z. Qureshi, S. Shahzadi. *Russ. J. Gen. Chem.*, **85**, 2183 (2015).
[6] H. Kargar. *Transition Met. Chem.*, **39**, 811 (2014).
[7] A.A. Dehghani-Firouzabadi, H. Kargar, S. Eslaminejad, B. Notash. *J. Coord. Chem.*, **68**, 4345 (2015).
[8] R. Kia, H. Kargar. *J. Coord. Chem.*, **68**, 1441 (2015).
[9] V. Torabi, H. Kargar, A. Akbari, R. Behjatmanesh-Ardakani, H. Amiri-Rudbari, M.N. Tahir. *J. Coord. Chem.*, **71**, 3748 (2018).
[10] K.S. Munawar, S. Ali, M.N. Tahir, N. Khalid, Q. Abbas, I.Z. Qureshi, S. Hussain, M. Ashfaq. *J. Coord. Chem.*, **73**, 2275 (2020).
[11] A. Rauf, A. Shah, K.S. Munawar, S. Ali, M.N. Tahir, M. Javed, A.M. Khan. *Arab. J. Chem.*, **13**, 1130 (2020).
[12] N. Raman, S.J. Raja, A. Sakthivel. *J. Coord. Chem.*, **62**, 691 (2009).
[13] B. Anupama, M. Padmaja, C.G. Kumari. *Eur. J. Chem.*, **9**, 389 (2012).
[14] G.S. Kurdekar, M. Sathisha, S. Budagumpi, N.V. Kulkarni, V.K. Revankar, D. Suresh. *Med. Chem. Res.*, **21**, 2273 (2012).
[15] A.P. Mishra, R. Mishra, R. Jain, S. Gupta. *Mycobiology*, **40**, 20 (2012).
[16] N. Kalarani, S. Sangeetha, P. Kamalakannan, D. Venkappayya. *Russ. J. Coord. Chem.*, **29**, 845 (2003).
[17] M. Shabbir, Z. Akhter, I. Ahmad, S. Ahmed, M. Shafiq, B. Mirza, V. McKee, K.S. Munawar, A.R. Ashraf. *J. Mol. Struct.*, **1118**, 250 (2016).
[18] S. Chandra, L.K. Gupta. *Spectrochim. Acta, Part A.*, **61**, 275 (2005).
[19] A. Rauf, A. Shah, K.S. Munawar, A.A. Khan, R. Abbasi, M.A. Yameen, A.M. Khan, A.R. Khan, I.Z. Qureshi, H.B. Kraatz. *J. Mol. Struct.*, **1145**, 132 (2017).
[20] W. Ahmad, S.A. Khan, K.S. Munawar, A. Khalid, S. Kawanl. *Trop. J. Pharm. Res.*, **16**, 1137 (2017).
[21] N. Raman, S. Sobha. *Spectrochim. Acta A. Mol. Biomol. Spectrosc.*, **85**, 223 (2012).
[22] P. Kumar, A.K. Singh, J.K. Saxena, D.S. Pandey. *J. Organomet. Chem.*, **694**, 3570 (2009).
[23] N. Raman, A. Sakthivel, M. Selvaganapathy, L. Mitu. *J. Mol. Struct.*, **1060**, 63 (2014).
[24] J. Joseph, K. Nagashri, G.A.B. Rani. *J. Saudi Chem. Soc.*, **17**, 285 (2013).
[25] *APEX2*, Bruker AXS Inc., Madison, WI (2013).
[26] G.M. Sheldrick. *Acta Crystallogr. A.*, **64**, 112 (2008).
[27] W. Parrish, J. Langford. International Tables for Crystallography, in: A.J.C. Wilson (Ed.), Kluwer, Dordrecht (1992).
[28] G.M. Sheldrick. *Acta Crystallogr.*, **C71**, 3 (2015).
[29] L.J. Farrugia. *J. Appl. Crystallogr.*, **45**, 849 (2012).
[30] *SAINT*, Bruker AXS Inc., Madison, WI (2013).
[31] A.L. Spek. *Acta Crystallogr. D. Biol. Crystallogr.*, **65**, 148 (2009).
[32] P.M. Selvakumar, E. Suresh, P.S. Subramanian. *Polyhedron*, **26**, 749 (2007).
[33] L.Q. Chai, Q. Hu, K.Y. Zhang, L.C. Chen, Y.X. Li, H.S. Zhang. *Appl. Organometal. Chem.*, **32**, e4426 (2018).
[34] T. Rosu, E. Pahontu, C. Maxim, R. Georgescu, N. Stanica, A. Gulea. *Polyhedron*, **30**, 154(2011).
[35] L. Zhou, Q. Hu, L.Q. Chai, K.H. Mao, H.S. Zhang. *Polyhedron*, **158**, 102 (2019).
[36] L.Q. Chai, L.J. Tang, K.Y. Zhang, J.Y. Zhang, H.S. Zhang. *Appl. Organomet. Chem.*, **31**, e3786 (2017).
[37] L.Q. Chai, L. Zhou, H.B. Zhang, K.H. Mao, H.S. Zhang. *New J. Chem.*, **43**, 12417 (2019).
[38] K. Zhao, Y. Qu, Y. Wu, C. Wang, K. Shen, C. Li, H. Wu. *Transit. Met. Chem.*, **44**, 713 (2019).
[39] S. Mao, H. Zhang, K. Shen, Y. Xu, X. Shi, H. Wu. *Polyhedron*, **134**, 336 (2017).
[40] L.Q. Chai, Q. Hu, K.Y. Zhang, L. Zhou, J.J. Huang. *J. Lumin.*, **203**, 234 (2018).
[41] C. Anitha, C.D. Sheela, P. Tharmaraj, S. Sumathi. *Spectrochim. Acta A. Mol. Biomol. Spectrosc.*, **96**, 493 (2012).
[42] T. Rosu, E. Pahontu, C. Maxim, R. Georgescu, N. Stanica, G.L. Almajan, A. Gulea. *Polyhedron*, **29**, 757 (2010).

[43] Y. Anjaneyulu, R.P. Rao. *Synth. React. Inorg. Met-Org. Chem.*, **16**, 257 (1986).
[44] B.G. Tweedy. *Phytopathology*, **55**, 910 (1964).
[45] N.A. Negm, M.F. Zaki, M.A.I. Salem. *Colloids Surf. B. Biointerfaces*, **77**, 96 (2010).
[46] A. Sahraei, H. Kargar, M. Hakimi, M.N. Tahir. *J. Mol. Struct.*, **1149**, 576 (2017).
[47] A. Sahraei, H. Kargar, M. Hakimi, M.N. Tahir. *Transit. Met. Chem.*, **42**, 483(2017).